1-1-2013

Microstructure and mechanical properties of 1050/6061 laminated composite processed by accumulative roll bonding

Lihong Su
University of Wollongong, lihongsu@uow.edu.au

Cheng Lu
University of Wollongong, chenglu@uow.edu.au

Guanyu Deng
University of Wollongong, gd577@uowmail.edu.au

A K. Tieu
University of Wollongong, ktieu@uow.edu.au

Xudong Sun
Northeastern University

Microstructure and mechanical properties of 1050/6061 laminated composite processed by accumulative roll bonding

Abstract

1050/6061 laminated composite sheets have been fabricated by the accumulative roll bonding (ARB) using commercial 1050 and 6061 aluminium alloys. Through-thickness hardness and tensile testes have been conducted to examine the mechanical properties of the laminated composites. It has been found that the strength of the composite materials is between the strengths of 6061 and 1050 primary materials. The average hardness of the 6061 layer is almost twice of the average value of the 1050 layer for both one and two-cycle processed composites. Optical microscopy, scanning electron microscopy and transmission electron microscopy were used to evaluate the microstructure of the composites. Grain refinement has been observed for both the 1050 and 6061 layers. The 1050 layer showed coarser and more equiaxed microstructure than the 6061 layer after the second ARB cycle.

Keywords

1050, 6061, laminated, composite, processed, accumulative, roll, bonding, mechanical, microstructure, properties

Disciplines

Engineering | Science and Technology Studies

Publication Details

Su, L., Lu, C., Deng, G., Tieu, A. K. & Sun, X. (2013). Microstructure and mechanical properties of 1050/6061 laminated composite processed by accumulative roll bonding. Reviews On Advanced Materials Science, 33 (1), 33-37.

Rev. Adv. Mater. Sci. 33 (2013) 33-37

MICROSTRUCTURE AND MECHANICAL PROPERTIES OF 1050/6061 LAMINATED COMPOSITE PROCESSED BY ACCUMULATIVE ROLL BONDING

Lihong Su[1,2], Cheng Lu[2], Guanyu Deng[2,3], Kiet Tieu[2] and Xudong Sun[1]

[1]School of Materials and Metallurgy, Northeastern University, Shengyang, China
[2]School of Mechanical, Materials and Methatronics, University of Wollongong, Australia
[3]State Key Lab of Rolling and Automation, Northeastern University, Shengyang, China

Received: October 17, 2011

Abstract. 1050/6061 laminated composite sheets have been fabricated by the accumulative roll bonding (ARB) using commercial 1050 and 6061 aluminium alloys. Through-thickness hardness and tensile testes have been conducted to examine the mechanical properties of the laminated composites. It has been found that the strength of the composite materials is between the strengths of 6061 and 1050 primary materials. The average hardness of the 6061 layer is almost twice of the average value of the 1050 layer for both one and two-cycle processed composites. Optical microscopy, scanning electron microscopy and transmission electron microscopy were used to evaluate the microstructure of the composites. Grain refinement has been observed for both the 1050 and 6061 layers. The 1050 layer showed coarser and more equiaxed microstructure than the 6061 layer after the second ARB cycle.

1. INTRODUCTION

Aluminium alloys have attracted much attention for their wide applications in automotive or aerospace industry. It's necessary to improve the properties of the aluminium alloys to widen their usage. Accumulative roll bonding (ARB) has become one of the most important severe plastic deformation (SPD) techniques since it was first introduced by Saito et al. [1]. As using the same equipment as conventional rolling, ARB is considered to be one of the most promising methods for manufacturing ultrafine grained sheet materials [2-4]. During ARB, rolling is conducted on two layered sheets which have the exact same dimensions and have been stacked together beforehand. The rolling process not only provides large plastic deformation but also has an effect of bonding the two layers together. The bonded specimen of each cycle is conducted to cutting, surface degreasing, brushing, and stacking together for the next cycle [1-2, 5-6]. The multi-layered materials obtained from ARB are quite different from materials manufactured by other SPD methods such as equal channel angular pressing (ECAP) or high pressure torsion (HPT) as the materials after ARB are more like a layered composite [5,7,8]. The process also allows bonding of two different kinds of materials and many studies have been done in this area [9-14].

In the current research, commercial aluminium alloys 1050 and 6061 have been used as primary materials in the ARB process to produce laminated composite materials. Since pure aluminium 1050 has good ductility and the 6061 alloy has high strength, the different properties of the two alloys would combine and enhance the mechanical properties of the composites [15].

Corresponding author: Cheng Lu, e-mail: chenglu@uow.edu.au

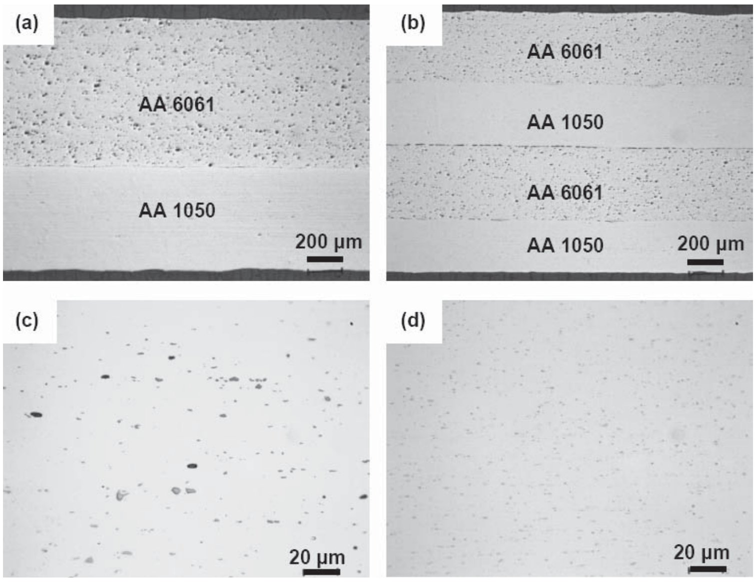

Fig. 1. Optical micrographs of the longitudinal cross section of specimens after (a) one-cycle (b) two-cycle ARB and (c) 6061 layer and (d) 1050 layer of the specimen after two-cycle ARB.

2. EXPERIMENTAL PROCEDURES

The materials used in this work were commercial aluminium alloy 1050 and 6061 sheets with initial thickness of 1.5 mm. The 1050 sheets were hot rolled state and the 6061 sheets were T6 treated. Vickers hardnesses of the 1050 and 6061 sheets were 44.1 and 102.7, respectively. The ARB samples were cut parallel to the original rolling direction, having the dimension of 1.5 mm × 50 mm × 400 mm (thickness×width×length). Prior to each rolling cycle, the roll was cleaned by acetone and the roll gap was set to the required setting. Two pieces of the original samples were degreased by acetone and wire-brushed. The samples were then stacked and heated in a furnace at 250 °C for 10 min and then rolled with a nominal reduction around 50% under dry condition. The rolled samples were cut into two halves and the edges were trimmed to avoid propagation of edge cracks. The above procedure proceeded for two ARB cycles.

The microstructure was observed by optical microscopy and transmission electron microscopy (TEM). The optical microstructures were observed with a Leica DMRM microscope, in the longitudinal cross-section after grinding and polishing with a Struer's TegraPol-21 polishing machine. TEM micrographs were obtained with a JEOL 2011F microscope operating at 200 kV. Thin foils for TEM were prepared by Plasma Ion Polishing with a Gatan 691 PIPS. Tensile tests were conducted with an Instron 1341 testing machine with an initial strain rate 10^{-3} /s at room temperature. Tensile specimens with 25 mm gauge length and 6 mm gauge width were processed along the rolling direction of the ARB processed samples. The fracture surfaces after tensile failure were observed by a JEOL 6490 scanning electron microscope. Vickers microhardness of the 6061 and 1050 layers in each cycle was measured with a Leco hardness testing machine by applying a load of 25 g for 12 s.

3. RESULTS AND DISCUSSION

Fig. 1 shows the optical microstructures observed at the TD (transverse direction) plane of the specimens produced by one- and two-cycle ARB. Good bonding with no delamination between the

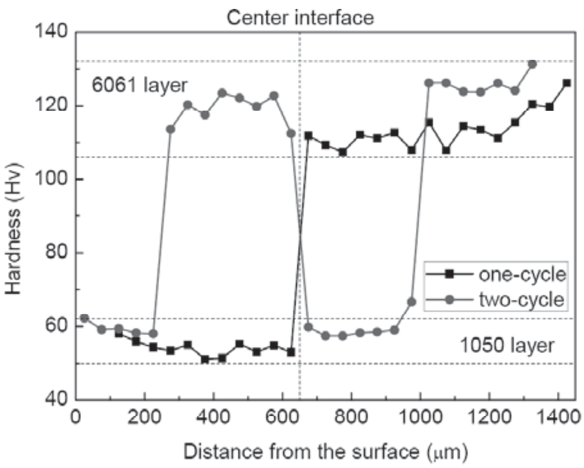

Fig. 2. Changes in Vickers hardness through the thickness of the specimens after one- and two-cycle ARB.

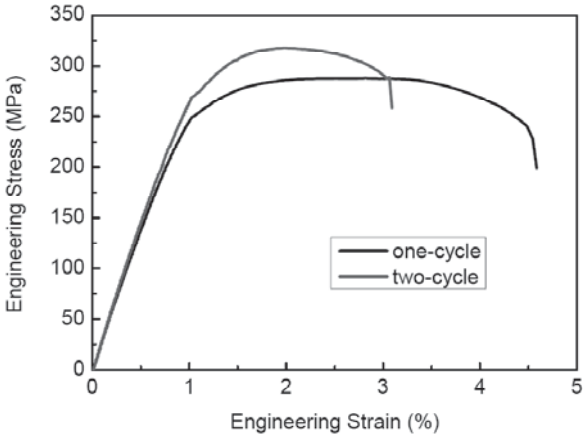

Fig. 3. Engineering stress-strain curves of the specimens after one- and two-cycle ARB.

sheets was attained at each cycle of ARB. The difference of the thickness of the two samples is due to the slightly variation of reduction during rolling and the loss of materials through wire brushing during the surface treatment. It can be seen from Figs. 1c and 1d that the 6061 layers show dense precipitates of Mg_2Si and Fe riched precipitates, whereas the 1050 layers are free of precipitates. The precipitates in 6061 layers were refined through ARB process, as can be seen from Figs. 1a and 1b. The 6061 layers are thicker than 1050 layers, which is due to the large difference of the hardness between the two primary materials. The softer materials are easier to deform resulting in a smaller volume fraction in the composite than the harder materials.

The through-thickness Vickers hardness of the one and two-cycle ARBed specimens is shown in Fig. 2. The average hardness of the 6061 layer is almost twice of the average value of the 1050 layer for both one and two-cycle processed materials. A clear jump at the interface is observed for both cycle indicating that the two materials are directly bonded and there is no transition region [15]. The hardness within the 1050 and 6061 layers is not homogeneous, having higher values near the surface. This behaviour was previously observed and was explained by the redundant shear strain near the surface [6]. It can be seen that the hardness value in the 6061 layer is more scattered than that in the 1050 layer, which is probably due to the dense precipitates in the 6061 layer that may cause inhomogeneous microstructure and hardness variation.

Tensile test results are shown in Fig. 3. After one-cycle ARB, the ultimate tensile strengths (UTS) of the composite material is about 288 MPa, which is slightly lower than the strength of the as-received 6061 alloy (330 MPa) and is more than twice of the

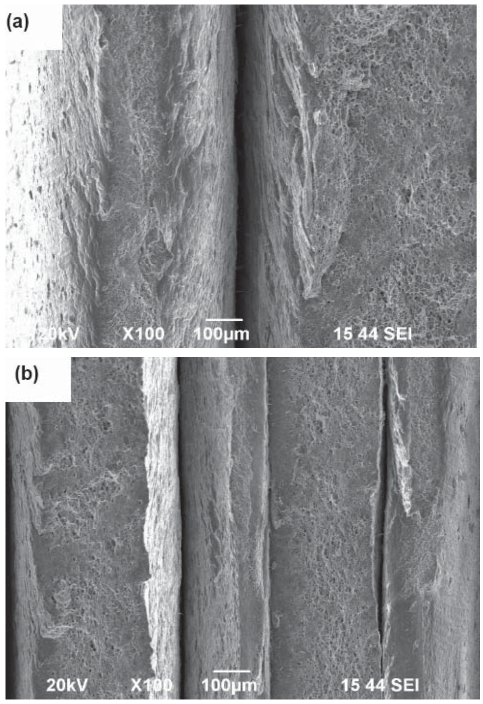

Fig. 4. Tensile fractographs of the specimens after (a) one- and (b) two-cycle ARB.

value of the 1050 primary materials (130 MPa). According to the rule of mixture (ROM), the tensile strength of the multi-layered composite is decided by the flow stresses of both constituents [16]. The strength of the composite materials from our experiments is between the strengths of 6061 and 1050 primary materials but closer to 6061 alloy, which is due to the larger volume fraction of 6061 alloy compared with 1050 alloy. After two-cycle ARB, the UTS of the composite material increased to 317 MPa. The total elongation after one-cycle ARB is about 4.5%, and then decreases to 3% after the second cycle.

The SEM micrographs of the fracture surfaces of one and two-cycle processed materials are shown in Fig. 4. It shows shear zones and dimples, which are the characteristics of ductile deformation. The interfaces can be clearly seen from the fracture surface, which is partly because of the shear zones between the interfaces and partly because of debonding during the tensile process. Because of the large hardness difference of the two primary materials, bonding becomes difficult and debonding is easy to occur during further deformation. Sandwich composites with the outside materials softer than the inside materials were used as primary materials by some researchers to avoid the bonding problem which allows all the bonding only between the soft materials [9-13]. A large amount of necking happened for the 1050 layer, compared to

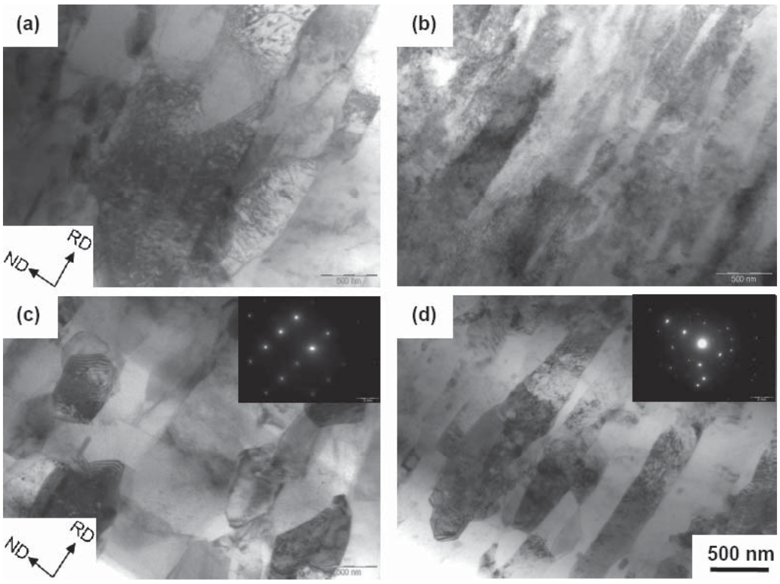

Fig. 5. TEM microstructure of (a) 1050 layer (b) 6061 layer after one-cycle ARB and (c) 1050 layer (d) 6061 layer after two-cycle ARB.

the 6061 layer, especially for the one-cycle processed sample, which means that the 1050 layer contributes a great deal to the elongation of the composite material. The necking of 1050 layers in the two-cycle processed sample seems to be smaller than the one-cycle sample, which indicates poorer ductility. This is in agreement with the tensile test results.

TEM microstructures observed at the cross section of the specimens processed by one- and two-cycle ARB are shown in Fig. 5. Figs. 5a and 5b show the microstructure of the 1050 and 6061 layer after one-cycle ARB. It is apparent that the microstructures of both the 1050 layer and the 6061 layer are consisted of strongly elongated subgrains with a band structure and are separated by low angle boundaries. The subgrain bands lie parallel to the rolling direction. The subgrain boundaries of the 1050 layer are more clearly defined than the 6061 layer, the microstructure of which consists of dense dislocations and it's hard to see any boundaries. Figs. 5c and 5d show the microstructure of the 1050 and 6061 layer after two-cycle ARB. As can be seen from the microstructure that the grain boundaries for both layers are much clearly defined and the grain sizes are smaller after the second cycle ARB than that of the first cycle. The grains of the 6061 layers are still strongly elongated in the rolling direction with a typical rolling microstructure with large aspect ratio. However, the microstructure of the 1050 layer appears equiaxed and is much coarser than the 6061 layer. The average grain thicknesses of the 1050 and 6061 layer are 550 nm and 200 nm, respectively. The SAD patterns were taken with an aperture of 20 μm in diameter. The diffraction pattern of 1050 layer is a single net pattern, whereas the 6061 layer shows a more complex and more diffused pattern, which approves the finer structure of the 6061 layer. The grain refinement from the first to the second cycle ARB is in good agreement with the strength and hardness increase as the strength of the ARB processed aluminium alloys is determined primarily by the ultra-fine grained structure [17]. Further annealing will be done to improve the ductility of the composite as the 1050 alloy is easier to have recovery than the 6061 alloy.

4. SUMMARY

1050/6061 laminated composites were produced by ARB and showed a combined strength of the two primary materials. After two-cycle ARB, the microstructure of ultrafine grains with clear grain boundaries has been obtained. The 1050 layer showed coarser and more equiaxed structure than the 6061 layer, which had a typical rolling structure with large aspect ratio banded grains. Debonding occurred during tensile tests which showed the difficulty of bonding two different materials with large hardness difference. Annealing before the ARB experiment and post ARB aging may be able to improve bonding and ductility.

ACKNOWLEDGEMENT

The authors acknowledge the financial support from an Australia Research Discovery Grant (DP773329).

The authors would like to thank Mr. Joe Abbott and Mr. Greg Tillman for experimental assistance. Lihong Su and Guanyu Deng would like to thank the financial support from China Scholarship Council (CSC).

REFERENCES

[1] Y. Saito, N. Tsuji, H. Utsunomiya, T. Sakai and R.G. Hong // *Scripta Mater.* **39** (1998) 1221.

[2] Y. Saito, H. Utsunomiya, N. Tsuji and T. Sakai // *Acta Mater.* **47** (1999) 579.

[3] M.Y. Zhan, Y.Y. Li, W.P. Chen and W.D. Chen // *J. Mater. Sci.* **42** (2007) 9256.

[4] R. Zhang and V.L. Acoff // *Mater. Sci. Eng. A* **463** (2007) 67.

[5] C. Lu, K. Tieu and D. Wexler // *J. Mater. Process. Tech*. **209** (2009) 4830.

[6] S.H. Lee, Y. Saito, T. Sakai and H. Utsunomiya // *Mater. Sci. Eng. A* **325** (2002) 228.

[7] R.Z. Valiev, R.K. Islamgaliev and I.V. Alexandrov // *Prog. Mater. Sci.* **45** (2000) 103.

[8] R.Z. Valiev, Y. Estrin, Z. Horita, T.G. Langdon, M.J. Zehetbauer and Y.T. Zhu // *JOM* **58** (2006) 33.

[9] M. Eizadjou, A.K. Talachi, H.D. Manesh, H.S. Shahabi and K. Janghorban // *Compos. Sci. Technol.* **68** (2008) 2003.

[10] S. Ohsaki, S. Kato, N. Tsuji, T. Ohkubo and K. Hono // *Acta Mater.* **55** (2007) 2885.

[11] G. Min, J. Lee, S. Kang and H. Kim // *Mater. Lett.* **60** (2006) 3255.

[12] M.C. Chen, H.C. Hsieh and W. Wu // *J. Alloy Compd.* **416** (2006) 169.

[13] K. Wu, H. Changa, E. Maawad, W.M. Gan, H.G. Brokmeier and M.Y. Zheng // *Mater. Sci. Eng. A* **527** (2010) 3073.

[14] F.H. Kavarana, K.S. Ravichandran and S.S. Sahay // *Scripta Mater.* **42** (2000) 949.

[15] T. Hausöl, H. W. Höppel and M. Göken // *J. Mater. Sci.* **45** (2010) 4733

[16] S.L. Lehoczky // *J. Appl. Phys.* **49** (1978) 5479.

[17] H. Kim, S. Kang, N. Tsuji and Y. Minamino // *Acta Mater.* **53** (2005) 1737.